Title: The fatty acids of sphingomyelins and ceramides in mammalian tissues and cultured cells: biophysical and physiological implications

Authors: Marco M. Manni, Jesús Sot, Enara Arretxe, Rubén Gil-Redondo, Juan M Falcón-Pérez, David Balgoma, Cristina Alonso, Félix M. Goñi, Alicia Alonso

PII: S0009-3084(18)30164-6
DOI: https://doi.org/10.1016/j.chemphyslip.2018.09.010
Reference: CPL 4686

To appear in: *Chemistry and Physics of Lipids*

Received date: 23-8-2018
Accepted date: 18-9-2018

Please cite this article as: Manni MM, Sot J, Arretxe E, Gil-Redondo R, Falcón-Pérez JM, Balgoma D, Alonso C, Goñi FM, Alonso A, The fatty acids of sphingomyelins and ceramides in mammalian tissues and cultured cells: biophysical and physiological implications, *Chemistry and Physics of Lipids* (2018), https://doi.org/10.1016/j.chemphyslip.2018.09.010

The fatty acids of sphingomyelins and ceramides in mammalian tissues and cultured cells: biophysical and physiological implications.

Marco M. Manni[1,2], Jesús Sot[1,2], Enara Arretxe[3], Rubén Gil-Redondo[4], Juan M Falcón-Pérez[4,5], David Balgoma[3], Cristina Alonso[3], Félix M. Goñi[1,2], and Alicia Alonso[1,2]*

[1]Instituto Biofisika (CSIC, UPV/EHU), Campus Universitario, 48940 Leioa, Spain.

[2]Departamento de Bioquímica, Universidad del País Vasco, B. Sarriena s/n, 48940 Leioa, Spain.

[3]OWL Metabolomics, Parque Tecnológico de Bizkaia, 48160, Derio, Spain

[4]CIC bioGUNE, CIBERehd, Parque Tecnológico de Bizkaia, 48160, Derio, Spain

[5]IKERBASQUE, Basque Foundation for Science, 48013, Bilbao, Spain

*Corresponding author. alicia.alonso@ehu.es

Highlights

- Lipidomic data of Cer and SM species in 35 mammalian tissues/cells are provided.
- The sphingoid base was predominantly d18-1 sphingosine in all cases.
- The most abundant Cer species were those containing C24:0 and C24:1 acyl chains.
- The main SM species was C16:0.
- Brain was an exception, with Cer and SM C18:0 as the main species.

Abstract

Sphingolipids consist of a sphingoid base N-linked to a fatty acyl chain. Among them, sphingomyelins (SM) are major components of mammalian cells, while ceramide (Cer) plays an important role as a lipid second messenger. We have performed a quantitative lipidomic study of Cer and SM species in different mammalian tissues (adipose tissue, liver, brain and blood serum of human, mice, rat and dog), as well as in cell cultures of mammalian origin (primary hepatocytes, immortalized MDCK cells, mice melanoma b16 cells, and mice primary CD4+ T lymphocytes) using an ultra-high performance liquid chromatography coupled to time-of-flight mass spectrometry (UHPLC-ToF-MS)-based platform. The data have been compared with published, in general semi-quantitative, results from 20 other samples, with good agreement. The sphingoid base was predominantly d18-1 sphingosine (2-amino-4-octadecene-1,3-diol) in all cases. The fatty acid composition of SM was clearly different from that of Cer. In virtually all

samples the most abundant Cer species were those containing C24:0 and C24:1 in their N-acyl chains, while the main species contained in SM was C16:0. Brain was the most divergent tissue, in which Cer and SM C18:0 were very abundant.

Keywords

Sphingolipids; sphingomyelins; ceramides; lipidomics; acyl chain composition

1. Introduction

Recent technical progress in organelle fractionation, mass spectroscopy, and the identification and characterization of most enzymes responsible for lipid synthesis has established that the lipid composition of cellular membranes varies significantly among organisms, tissues, and organelles (Antonny et al., 2015). These differences are probably related to specific structural and physiological properties of the different cells, tissues and organs. In this context lipid compositions were until now mainly analyzed considering the lipid species and classified according to their polar head. Using this criterion phospholipids have been generally classified as phosphatidylcholines (PC), phosphatidylethanolamines (PE), phosphatidylserines (PS), phosphatidylinositols (PI), sphingomyelins (SM) and phosphatidic acids (PA) (Van Meer et al., 2008). More recently the current lipidomic improvements have allowed the study of the specific acyl chains associated to each phospholipid species (Ejsing et al., 2009; Han, 2016; Shaner et al., 2009; Zheng et al., 2006), with the possibility of relating those data to specific biophysical properties of each lipid.

Sphingolipids appear mainly in eukaryotic cells, where they exert important structural and signalling functions (Hannun and Obeid, 2017). Sphingolipids are also known for their unusual biophysical properties (Carrer and Maggio, 1999). Among them ceramides (Cer) and sphingomyelins (SM), which are metabolically inter-related (Fig. 1), are particularly interesting because they exert very different functional roles.

Apart from being important intermediates in sphingolipid metabolism, Cer play an important role as lipid second messengers, or metabolic signals. A large number of agonists and stress signals induce the hydrolysis of SM and/or other changes in sphingolipid metabolism that are accompanied by the accumulation of Cer (Hannun and Luberto, 2000). Ceramides are structurally organised around a sphingoid base, one of a set of aliphatic amino alcohols of which the most abundant is sphingosine (d18:1). Sphingosine is N-linked via an amide linkage to a fatty acyl chain, with a varying length from 2 to 34 carbons and different degrees of unsaturation and hydroxylation (Furland et al., 2007; Poulos et al., 1987). Cer structure entails unique biophysical properties leading to a special behaviour in membranes. Indeed, very low concentrations of them suffice to form a Cer-enriched gel phase by lateral segregation in the presence of a vast excess of membrane phospholipids (Veiga et al., 1999). Moreover Cer have been proposed to play an important role in apoptosis, i.e. programmed cell death. This might be related to their unusual property of increasing the permeability of model and cell membranes, both to small and large, protein-sized, macromolecules (Artetxe et al., 2017; Montes et al., 2002; Ruiz-Argüello et al., 1996). Perhaps, because of their potent membrane-

perturbing properties, Cer exist in very low concentrations in cell membranes (< 1 mol% lipid), except under stress conditions, when their concentration may increase by one order of magnitude (Kolesnick et al., 2000). Cer also appears to be a lipotoxic component in mouse and human plasma, liver and adipose tissue, and its levels increase after a fat diet (Heilbronn et al., 2013; Holland et al., 2011; Rodriguez-Cuenca et al., 2017).

In contrast, SM are major components of mammalian cells (10-20 mol% of plasma membrane lipids). They consist of a hydrophobic Cer backbone with a phosphorylcholine esterified through its C1-OH (the N-acyl chain contains typically 16-24 carbon atoms). SM have a strong tendency to form stable bilayers in aqueous media. In addition, they interact with cholesterol and with ceramides, presumably through multiple hydrogen bonds, giving rise to lateral heterogeneities ('domains') in membranes. Biologically, SM are involved in different physiological processes such as endocytosis and receptor-mediated ligand uptake, ion channel and G-protein coupled receptor function, and protein sorting. SM are also an important constituent of the eye lens membrane, and they are believed to participate in the regulation of various nuclear functions (Slotte, 2013).

In spite of extensive studies on the biophysical properties of Cer and SM (García-Arribas et al., 2016; Goñi and Alonso, 2006) the relevance of the N-acyl chains for those properties has not been addressed in detail (see review in (Alonso and Goñi, 2018)). Sot et al. (2005), compared the properties of short-, medium-, and long-chain Cer. Pinto et al. (2008) inaugurated the studies of very long-chain ceramides with their data on C24:1. Contreras et al. (Contreras et al., 2012) described the specificity of C18:0 SM in the binding to the transmembrane domain of the COPI machinery protein p24. Jimenez-Rojo et al. (2014) published the thermotropic properties of SM, Cer, and SM-Cer mixtures with different N-acyl chain lengths. All these studies underline the importance of the N-acyl chain in the sphingolipid biophysical properties. Even so, there are very few detailed, reliable studies on the N-acyl chain composition of Cer or SM depending on the natural origin, and the vast majority of the biophysical investigations have been carried out with the C16:0 N-acyl derivatives, as representatives of the physiological molecules. It is somewhat surprising that the modern lipidomics techniques have hardly been specifically applied to examine the N-acyl contents of sphingolipids. Exceptions to this rule, such as the detailed study of Cer and SM species in cultured human fibroblasts and rat cerebellar granule cells performed by Valsecchi et al. (2007), are discussed below.

The present contribution intends to fill in the gap of quantitative lipidomic studies of natural origin sphingolipids and describes the results of a lipidomic study of SM and Cer species in different mammalian tissues (adipose tissue, liver, brain and blood serum of human, mice, rat and dog), as well as in cell cultures of mammalian origin (primary hepatocytes, immortalized MDCK cells, mice melanoma B16 cells, and mice primary CD4+ T lymphocytes). An ultra-high performance liquid chromatography coupled to time-of-flight mass spectrometry (UHPLC-ToF-MS)-based platform was used for optimal profiling of the lipidome.

2. Materials and methods

2.1 Materials

All human (male and female) serum/tissue donors were healthy, with normal levels of cholesterol and triglycerides, no diabetes and no drug treatment. Ages were between 20 and 50, about equal number of samples per decade. Serum and tissue samples of healthy volunteers included in this study (with informed consent) were provided by the Basque

Biobank for Research-OEHUN (http://www.biobancovasco.org/) and were processed with appropriate approval of the Ethics Committee. All methods were carried out in accordance with relevant guidelines and regulations and all experimental protocols were approved by the Biobank Ethics Committee.

Standards for mass spectrometry were supplied by Avanti Polar Lipids (Alabaster, AL, USA). Organic solvents were spectroscopic grade.

2.2 Lipid extraction from cell cultures

Proteins were precipitated from lysed cell samples (10-15 million cells) by adding 600 µl methanol and 450 µl chloroform. Samples were incubated at 20°C for 30 min and, after vortex, a 500 µl aliquot was collected and mixed with 75 µl water (pH 9). After brief vortex mixing, the samples were incubated for 1 h at 20°C. After centrifugation at 16,000 x g and 4°C for 15 min, 180 µl of the organic phase was collected and the solvent removed. The dried extracts were then reconstituted in 50 µl acetronitrile/isopropanol (1:1), resuspended for 10 min, centrifuged (16,000 x g for 5 minutes at 4 °C), and transferred to vials for UHPLC–MS analysis (Manni et al., 2017).

2.3 Lipid extraction from tissues

Approximately 15 mg of each tissue are weighted for the lipid extraction. Proteins were precipitated by adding sodium chloride (50 mM) (3:1, v/w) and chloroform/methanol (2:1) (30:1, v/w). The homogenization of the resulting mixture was then performed using a Precellys 24 homogenizer (Bertin Instruments, Montigny-le-Bretonneux, France) at 6500 rpm for 45 seconds. Samples were incubated at -20 ˚C for 1 hour and after vortexing them, 500 µl were collected. After centrifugation at 18,000 x g for 15 minutes at 4 °C, the organic phase was collected and dried under vacuum. Dried extracts were then reconstituted in acetronitrile/isopropanol (1:1), resuspended with agitation for 10 minutes, centrifuged (16,000 x g for 5 minutes at 4 °C), and transferred to plates for UHPLC-MS analysis (Manni et al., 2017).

2.4 Lipid extraction from serum

10 µl of serum were mixed with sodium chloride (50 mM) and chloroform/methanol (2:1) in 1.5 mL microtubes at room temperature. After brief vortex mixing, the samples were incubated for 1 hour at -20 ˚C. After centrifugation at 16,000 x g for 15 minutes at 4 °C, the organic phase was collected and the solvent removed under vacuum. The dried extracts were then reconstituted in 100 µl acetronitrile / isopropanol (1:1), centrifuged (16,000 x g for 5 minutes at 4 °C), and transferred to vials for UHPLC-MS analysis (Manni et al., 2017).

2.5 UHPLC-MS analysis

Analysis was performed using the ACQUITY UPLC® system (Waters Corp., Milford, MA, USA) coupled online to a Waters QTOF PremierTM (Waters Corp.) with a 2.1 × 100 mm ACQUITY 1.7 m C18 BEH column (Waters Corp.) maintained at 60 °C. The mobile phase, at a flow rate of 0.15 mL/min, initially consisted of 60% solvent A (water, acetonitrile, and 10mM ammonium formate) and 40% solvent B (acetonitrile, isopropanol, and 10mM ammonium formate), increasing to 100% B over 10 minutes. After 5 minutes the mobile phase was reset to the initial composition in readiness for the subsequent injection which proceeded a 45 s system recycle time. The volume of sample injected onto the column was 2 µL. Mass spectrometry was used in positive ion modes with the capillary current set at 2000 V and the cone voltages at 30 V. The nebulizer gas was set at a flow rate of 1000 L/h and a temperature of 400 °C and the cone

gas at a flow rate of 30 L/h and a source temperature of 120 °C (Barr et al., 2012; Martínez-Uña et al., 2013).

Data were acquired in centroid mode at a resolution of 12000, using an accumulation time of 0.2 s per spectrum. MS data were acquired over an m/z range 50-1000. All spectra were mass-corrected in real time by reference to leucine enkephalin, infused at a constant flow rate of 50 µL/ min (external pump) through an independent reference electrospray. The frequency was set at 10 s. A single lock mass calibration at m/z 556.2771 in positive ion mode was used for the complete analysis. The system was controlled by Masslynx 4.1 (Waters Corp.). The overall quality of the analysis procedure was monitored using six repeat injections of a pooled sample, considered as the quality control sample. Generally, the retention time stability was < 6 s injection-to-injection variation and the mass accuracy < 3 ppm for m/z 400-1200, and < 1.2 mDa for m/z 50-400. The ion features considered for the following data analysis of the sphingolipid classes were the adducts $[M+H]^+$ for sphingomyelins and $[M+H-H2O]^+$ for ceramides, where M+H corresponds to the analyte molecule.

2.6 Number of samples for MS analysis

Number of samples was: human adipose tissue, 68; rat adipose tissue, 5; rat brain, 5; mouse brain, 5; canine liver, 3; healthy human liver, 8; rat liver, 5; mouse liver, 10; healthy human serum, 285; rat serum, 5; mouse serum, 10; primary hepatocytes, 10; mouse lymphocytes isolated from peripheral blood, 3; B16 cells, 20.

2.7 Sphingolipid quantification

Quantification was achieved by external calibration considering linear and quadratic calibration. Briefly, the calibration curve was prepared by weighing 5 mg of the appropriate standards (Avanti, Alabaster, AL, USA) and preparing solutions in volumetric flasks with methanol. From a mixture prepared in a volumetric flask, serial dilutions were done. In all cases it was assumed that the recovery of extraction was 100%. Concentration ranges were calculated with 95% interval of confidence assuming t-distribution. Data are given per mg fresh weight tissue or per mL in the case of serum.

3. Results

This study describes the SM and Cer composition of different mammalian tissues and cell cultures through liquid chromatography coupled to mass spectrometry. Fig. 2 shows a 'heatmap' summarizing the detected SM and Cer species in the various tissues/cells. The quantitative data can be found in the Supplementary Material. The sphingoid base was predominantly d18-1 sphingosine (2-amino-4-octadecene-1,3-diol). The most abundant Cer species were those containing C24:1 and C24:0 as their N-acyl chains. The distribution was very similar in all tissues, except in brain, that contains C18:0 as the main species. No major changes were observed among different organisms, but for the higher levels of C22:0 Cer detected in mice liver and serum. The results in cells were similar to those observed in tissues, with a clear predominance of C24:1 and C24:0 Cer.

However, with respect to SM the data in Fig. 2 show a predominance of C16:0, followed by C24:1 and C24:0 for most of the tissues and cells. Again, the brain showed a substantial presence of C18:0, with relatively lower levels of C16:0.

Absolute values, rather than percent distributions, were obtained for selected lipids and tissues through the use of quantitative internal standards. The results are summarized in Table 1. In all cases total SM concentration is at least one order of magnitude higher than the total Cer concentration, as expected for the extreme Cer activity in destabilizing membrane structure (Contreras et al., 2005; Ruiz-Argüello et al., 1996). The most abundant Cer in all samples is C24:0, except in brain where C18:0 predominates. In turn the N-acyl C16:0 chain, a minor presence in Cer, is the most abundant one in SM (together with C24:0 in liver and brain).

4. Discussion

The overall conclusion of our lipidomic studies is that, in spite of their close metabolic kinship, the fatty acid composition of SM is clearly different from that of Cer. Possible explanations include the fact that ceramide may arise not only from sphingomyelinase cleavage of SM, e.g. under stress conditions, but also from de novo synthesis by the ceramide synthases (Levy and Futerman, 2010; Mullen et al., 2011). In any case a poorly known interplay of esterases and synthases could also remodel the fatty acid compositions of SM and Cer.

In agreement with published data, our analysis show that the sphingoid base was predominantly d18-1 sphingosine (2-amino-4-octadecene-1,3-diol) (Kolak et al., 2007; Sugimoto et al., 2016; Valsecchi et al., 2007; Zhang et al., 2013). In other hands our quantification showed that in all cases total SM concentration is at least one order of magnitude higher than the total Cer concentration. This trend was also observed in other studies (Kolak et al., 2007; Valsecchi et al., 2007; Zhang et al., 2013) and it is expected from the extreme Cer activity in destabilizing membrane structure (Alonso and Goñi, 2018; Goñi et al., 2014).

An important general observation is the fact that C16:0 predominates in SM, while C24:0 does so in Cer. These two fatty acids differ fundamentally in the length. C16:0 fits well the thickness of a half-bilayer, while C24:0 is far too long. SM is essentially a structural lipid that stabilizes the membrane bilayer, thus the abundance of C16:0 is very appropriate for its role. Studies by Jiménez-Rojo et al. (2014) show that the thermotropic gel-fluid transition of C16:0 SM is very narrow, i.e. highly cooperative, as occurs with the fully saturated glycerophospholipids (Marsh, 2013), while C24:0 SM gives rise to a complex endothermic signal, indicative of bilayer heterogeneities, probably due to N-acyl chain interdigitation between both monolayers. Supporting the results above, Maté et al. (2014) described that C24:0 SM and C16:0 SM gave rise to lateral segregation and domain formation in ternary mixtures with dioleoyl phosphatidylcholine. In contrast C24:1 SM and C16:0 SM were miscible, giving rise to a homogeneous phase.

With respect to ceramides, the abundance of C24 species is very remarkable (Table 1) and is in contrast with the predominant use of C16:0 Cer in most biophysical and biochemical studies. An exception to the latter rule is constituted by the studies of Jimenez-Rojo et al. (2014), Pinto et al. (2008, 2011) including C24 Cer, and the series of reports by Slotte and co-workers (Al Sazzad et al., 2017; Ekholm et al., 2011; Maula et al., 2015; Maula et al., 2012; Slotte, 2013) in which both the polar and non-polar parts of sphingolipids are systematically varied. Pinto et al. (2008, 2011) found that C18:0 Cer and C24:0 Cer had several biophysical properties in common, except for the latter's tendency to form tubular structures in giant unilamellar vesicles when mixed with palmitoyl oleoyl phosphatidylcholine. Tubulation was hypothetically

related by those authors to the acyl chain length asymmetry and subsequent packing defects caused by the interdigitation of the C24 chain.

Results from other laboratories concerning the Cer and SM species in natural tissues are summarized in Table 2. Although quantitative data are not very common, mass spectrometry being used primarily to obtain percent distributions of lipid species, at least the most abundant species in each examined system can be easily detected, and they are included in Table 2. There is good agreement between our data in Fig. 2 and those in Table 2. The predominance of C16:0 as the main fatty acid in SM is widespread, with the exception of nervous and muscle tissues, where C18:0 SM predominates. The complex relationship between SM C16:0. C24:0 and C24:1, described in (Maté et al., 2014) and discussed above may explain the frequent coexistence of saturated and unsaturated SM. Of 15 samples (Tables 1 and 2) in which C16:0 is the predominant SM species, SM C24:1 is also found among the most abundant SM species in 11 of them.

Some more variation exists in ceramide. Of 31 Cer samples whose fatty acyl data are known from the combined Fig. 2 and Table 2, C24:0 was the most abundant species in 17 of them, while C24:1 predominated in 7. Only in two samples (human adipose tissue and exosomes from human prostate cancer cells) was Cer C16:0 found as the main species. Again C18:0 was mainly found in nervous and muscle tissues.

Our observation that C18:0 SM and C24:1 SM were the most abundant species in brain (Fig. 2, Table 1) deserves some comment. C18:0 SM was also the most abundant species found by Takamori et al. (Takamori et al., 2006) in synaptic vesicles. In the same study the authors detected as well a high percentage of polyunsaturated phospholipids and an enrichment in cholesterol. In this context, considering the low affinity of polyunsaturated lipids for colesterol (Ipsen et al., 1987), C18:0 SM could participate actively interacting with the sterol and giving rise to specific fluid-ordered domains. Moreover the high levels of C24:1 in brain (Fig. 2) could be related to its fluidifying tendency (Maté et al., 2014), and this could find an application in the synaptic regions in which a high fluidity is needed to facilitate exocytosis and membrane recycling. In a recent contribution Manni et al. (2018) described that polyunsaturated phospholipids confer to biological membranes special mechanical properties increasing the ability of dynamin to cause fission, probably for the high flexibility of their acyl chains.

Valsecchi et al. (2007) also found that C18:0 was the most abundant species in Cer and SM of rat cerebellar cultured cells while C16:0 and C24:1 predominated in cultured fibroblasts. However, at variance with those authors, we found a relative abundance of SM species with fatty acids longer than C18 in brain SM, mainly C24:0 and C24:1. Our quantitative results for brain tissue are in good agreement with those by Valsecchi et al. (2007) for cerebellar cultured neurons. (For comparing the latter and our own results we have assumed that the examined tissues contained about 100 µg protein/mg wet wt tissue).

The physiological correlations of these data are not easy to establish. However, Hartmann et al. (Hartmann et al., 2012; Hartmann et al., 2013) demonstrated that in human colon and breast cancer cells, overproduction of C16:0 or C18:0 Cer induces apoptosis and inhibits cell cycle progression, leading to inhibition of cell proliferation and cell death. On the other hand, overproduction of very long chain Cer (d18:1/24:0-24:1) had a slight proliferative effect in these cells. These data could give us an indication about the importance of the balance of chain length in cell physiology. The tendency detected in our study seems to relate the abundance of very long chain with actively proliferating cells, as liver cells, primary

hepatocytes and cultured cell lines. However, in neurons, which are well known not to undergo cell division in the adult brain, C18:0 Cer is the most abundant species.

Our contribution constitutes a detailed study about Cer and SM species in different organisms and tissues taking advantage of available metabolomic data (Martínez-Arranz et al., 2015). We detected that sphingolipid species are conserved in different mammals while no organism-specificity was observed. The most divergent tissue was brain, probably for its structural and functional peculiarities. While SM are well known to be important in the stability and structural integrity of plasma membrane, Cer are considered for their importance as signaling mediators in the balance between cell death and proliferation. For this reason, several studies have been published relating imbalance of Cer and SM lipid species to various diseases. In this context our study opens an interesting issue about the involvement of sphingolipid species in the physiology of cells. It also demands an effort in the biophysical studies of the largely neglected C18-C24 sphingolipids.

Acknowledgements

This work was supported in part by grants from the Spanish Government (FEDER MINECO BFU 2015-66306-P) and the Basque Government (IT849-13 to F.M.G. and IT838-13 to A.A.). M.M.M. was a pre-doctoral fellow of the Basque government.

Authors Contribution

M.M.M., J.S., C.A., F.M.G. and A.A. designed the study and wrote the manuscript, E.A., R.G.R., J.M.F.P., D.B. and C.A. performed and/or supervised the measurements, all authors discussed the results.

Additional Information

Competing Financial Interests: The authors claim no competing financial interests with this publication.

Supplementary information is provided.

References

Al Sazzad, M.A., Yasuda, T., Murata, M., Slotte, J.P., 2017. The Long-Chain Sphingoid Base of Ceramides Determines Their Propensity for Lateral Segregation. Biophysical journal 112, 976-983.

Alonso, A., Goñi, F.M., 2018. The Physical Properties of Ceramides in Membranes. Annual review of biophysics 47, 633-654.

Antonny, B., Vanni, S., Shindou, H., Ferreira, T., 2015. From zero to six double bonds: phospholipid unsaturation and organelle function. Trends in cell biology 25, 427-436.

Artetxe, I., Ugarte-Uribe, B., Gil, D., Valle, M., Alonso, A., García-Sáez, A.J., Goñi, F.M., 2017. Does ceramide form channels? The ceramide-induced membrane permeabilization mechanism. Biophysical journal 113, 860-868.

Barr, J., Caballería, J., Martínez-Arranz, I., Domínguez-Díez, A., Alonso, C., Muntané, J., Pérez-Cormenzana, M., García-Monzón, C., Mayo, R., Martín-Duce, A., 2012. Obesity-dependent metabolic signatures associated with nonalcoholic fatty liver disease progression. Journal of proteome research 11, 2521-2532.

Carrer, D.C., Maggio, B., 1999. Phase behavior and molecular interactions in mixtures of ceramide with dipalmitoylphosphatidylcholine. Journal of lipid research 40, 1978-1989.

Contreras, F.-X., Basañez, G., Alonso, A., Herrmann, A., Goñi, F.M., 2005. Asymmetric addition of ceramides but not dihydroceramides promotes transbilayer (flip-flop) lipid motion in membranes. Biophysical journal 88, 348-359.

Contreras, F.-X., Ernst, A.M., Haberkant, P., Björkholm, P., Lindahl, E., Gönen, B., Tischer, C., Elofsson, A., von Heijne, G., Thiele, C., 2012. Molecular recognition of a single sphingolipid species by a protein's transmembrane domain. Nature 481, 525.

Dautel, S.E., Kyle, J.E., Clair, G., Sontag, R.L., Weitz, K.K., Shukla, A.K., Nguyen, S.N., Kim, Y.-M., Zink, E.M., Luders, T., 2017. Lipidomics reveals dramatic lipid compositional changes in the maturing postnatal lung. Scientific reports 7, 40555.

Ejsing, C.S., Sampaio, J.L., Surendranath, V., Duchoslav, E., Ekroos, K., Klemm, R.W., Simons, K., Shevchenko, A., 2009. Global analysis of the yeast lipidome by quantitative shotgun mass spectrometry. Proceedings of the National Academy of Sciences 106, 2136-2141.

Ekholm, O., Jaikishan, S., Lönnfors, M., Nyholm, T.K., Slotte, J.P., 2011. Membrane bilayer properties of sphingomyelins with amide-linked 2-or 3-hydroxylated fatty acids. Biochimica et Biophysica Acta (BBA)-Biomembranes 1808, 727-732.

Furland, N.E., Oresti, G.M., Antollini, S.S., Venturino, A., Maldonado, E.N., Aveldaño, M.I., 2007. Very long-chain polyunsaturated fatty acids are the major acyl groups of sphingomyelins and ceramides in the head of mammalian spermatozoa. Journal of Biological Chemistry 282, 18151-18161.

García-Arribas, A.B., Alonso, A., Goñi, F.M., 2016. Cholesterol interactions with ceramide and sphingomyelin. Chemistry and physics of lipids 199, 26-34.

Goñi, F.M., Alonso, A., 2006. Biophysics of sphingolipids I. Membrane properties of sphingosine, ceramides and other simple sphingolipids. Biochimica et Biophysica Acta (BBA)-Biomembranes 1758, 1902-1921.

Goñi, F.M., Sot, J., Alonso, A., 2014. Biophysical properties of sphingosine, ceramides and other simple sphingolipids. Portland Press Limited.

Han, X., 2016. Lipidomics: Comprehensive mass spectrometry of lipids. John Wiley & Sons.

Hannun, Y.A., Luberto, C., 2000. Ceramide in the eukaryotic stress response. Trends in cell biology 10, 73-80.

Hannun, Y.A., Obeid, L.M., 2017. Sphingolipids and their metabolism in physiology and disease. Nature reviews Molecular cell biology.

Hartmann, D., Lucks, J., Fuchs, S., Schiffmann, S., Schreiber, Y., Ferreirós, N., Merkens, J., Marschalek, R., Geisslinger, G., Grösch, S., 2012. Long chain ceramides and very long chain ceramides have opposite effects on human breast and colon cancer cell growth. The international journal of biochemistry & cell biology 44, 620-628.

Hartmann, D., Wegner, M.-S., Wanger, R.A., Ferreirós, N., Schreiber, Y., Lucks, J., Schiffmann, S., Geisslinger, G., Grösch, S., 2013. The equilibrium between long and very long chain ceramides is important for the fate of the cell and can be influenced by co-expression of CerS. The international journal of biochemistry & cell biology 45, 1195-1203.

Heilbronn, L.K., Coster, A.C., Campbell, L.V., Greenfield, J.R., Lange, K., Christopher, M.J., Meikle, P.J., Samocha-Bonet, D., 2013. The effect of short-term overfeeding on serum lipids in healthy humans. Obesity 21.

Holland, W.L., Miller, R.A., Wang, Z.V., Sun, K., Barth, B.M., Bui, H.H., Davis, K.E., Bikman, B.T., Halberg, N., Rutkowski, J.M., 2011. Receptor-mediated activation of ceramidase activity initiates the pleiotropic actions of adiponectin. Nature medicine 17, 55.

Ipsen, J.H., Karlström, G., Mourtisen, O., Wennerström, H., Zuckermann, M., 1987. Phase equilibria in the phosphatidylcholine-cholesterol system. Biochimica et Biophysica Acta (BBA)-Biomembranes 905, 162-172.

Jimenez-Rojo, N., Garcia-Arribas, A.B., Sot, J., Alonso, A., Goni, F.M., 2014. Lipid bilayers containing sphingomyelins and ceramides of varying N-acyl lengths: a glimpse into sphingolipid complexity. Biochimica et Biophysica Acta (BBA)-Biomembranes 1838, 456-464.

Kolak, M., Westerbacka, J., Velagapudi, V.R., Wågsäter, D., Yetukuri, L., Makkonen, J., Rissanen, A., Häkkinen, A.-M., Lindell, M., Bergholm, R., 2007. Adipose tissue inflammation and increased ceramide content characterize subjects with high liver fat content independent of obesity. Diabetes 56, 1960-1968.

Kolesnick, R.N., Goñi, F.M., Alonso, A., 2000. Compartmentalization of ceramide signaling: physical foundations and biological effects. Journal of cellular physiology 184, 285-300.

Kosinska, M.K., Liebisch, G., Lochnit, G., Wilhelm, J., Klein, H., Kaesser, U., Lasczkowski, G., Rickert, M., Schmitz, G., Steinmeyer, J., 2014. Sphingolipids in human synovial fluid-a lipidomic study. PloS one 9, e91769.

Lazzarini, A., Macchiarulo, A., Floridi, A., Coletti, A., Cataldi, S., Codini, M., Lazzarini, R., Bartoccini, E., Cascianelli, G., Ambesi-Impiombato, F.S., 2015. Very-long-chain fatty acid sphingomyelin in nuclear lipid microdomains of hepatocytes and hepatoma cells: can the exchange from C24: 0 to C16: 0 affect signal proteins and vitamin D receptor? Molecular biology of the cell 26, 2418-2425.

Levy, M., Futerman, A.H., 2010. Mammalian ceramide synthases. IUBMB life 62, 347-356.

Llorente, A., Skotland, T., Sylvänne, T., Kauhanen, D., Róg, T., Orłowski, A., Vattulainen, I., Ekroos, K., Sandvig, K., 2013. Molecular lipidomics of exosomes released by PC-3 prostate cancer cells. Biochimica et Biophysica Acta (BBA)-Molecular and Cell Biology of Lipids 1831, 1302-1309.

Manni, M.M., Cano, A., Alonso, C., Goñi, F.M., 2015. Lipids that determine detergent resistance of MDCK cell membrane fractions. Chemistry and physics of lipids 191, 68-74.

Manni, M.M., Tiberti, M.L., Pagnotta, S., Barelli, H., Gautier, R., Antonny, B., 2018. Acyl chain asymmetry and polyunsaturation of brain phospholipids facilitate membrane vesiculation without leakage. eLife 7, e34394.

Manni, M.M., Valero, J.G., Pérez-Cormenzana, M., Cano, A., Alonso, C., Goñi, F.M., 2017. Lipidomic profile of GM95 cell death induced by Clostridium perfringens alpha-toxin. Chemistry and physics of lipids 203, 54-70.

Marsh, D., 2013. Handbook of lipid bilayers. CRC press.

Martínez-Arranz, I., Mayo, R., Pérez-Cormenzana, M., Mincholé, I., Salazar, L., Alonso, C., Mato, J.M., 2015. Enhancing metabolomics research through data mining. Journal of proteomics 127, 275-288.

Martínez-Uña, M., Varela-Rey, M., Cano, A., Fernández-Ares, L., Beraza, N., Aurrekoetxea, I., Martínez-Arranz, I., García-Rodríguez, J.L., Buqué, X., Mestre, D., 2013. Excess S-adenosylmethionine reroutes phosphatidylethanolamine towards phosphatidylcholine and triglyceride synthesis. Hepatology 58, 1296-1305.

Maté, S., Busto, J.V., García-Arribas, A.B., Sot, J., Vazquez, R., Herlax, V., Wolf, C., Bakás, L., Goni, F.M., 2014. N-Nervonoylsphingomyelin (c24: 1) prevents lateral heterogeneity in cholesterol-containing membranes. Biophysical journal 106, 2606-2616.

Maula, T., Al Sazzad, M.A., Slotte, J.P., 2015. Influence of hydroxylation, chain length, and chain unsaturation on bilayer properties of ceramides. Biophysical journal 109, 1639-1651.

Maula, T., Artetxe, I., Grandell, P.-M., Slotte, J.P., 2012. Importance of the sphingoid base length for the membrane properties of ceramides. Biophysical journal 103, 1870-1879.

Mecatti, G.C., Fernandes Messias, M.C., Sant'Anna Paiola, R.M., Figueiredo Angolini, C.F., da Silva Cunha, I.B., Eberlin, M.N., de Oliveira Carvalho, P., 2018. Lipidomic profiling of plasma and erythrocytes from septic patients reveals potential biomarker candidates. Biomarker insights 13, 1177271918765137.

Montes, L.R., Ruiz-Argüello, M.B., Goñi, F.M., Alonso, A., 2002. Membrane restructuring via ceramide results in enhanced solute efflux. Journal of Biological Chemistry 277, 11788-11794.

Montgomery, M.K., Brown, S.H., Mitchell, T.W., Coster, A.C., Cooney, G.J., Turner, N., 2017. Association of muscle lipidomic profile with high-fat diet-induced insulin resistance across five mouse strains. Scientific Reports 7, 13914.

Mullen, T.D., Jenkins, R.W., Clarke, C.J., Bielawski, J., Hannun, Y.A., Obeid, L.M., 2011. Ceramide Synthase-dependent Ceramide Generation and Programmed Cell Death INVOLVEMENT OF SALVAGE PATHWAY IN REGULATING POSTMITOCHONDRIAL EVENTS. Journal of Biological Chemistry 286, 15929-15942.

Pinto, S.N., Silva, L.C., De Almeida, R.F., Prieto, M., 2008. Membrane domain formation, interdigitation, and morphological alterations induced by the very long chain asymmetric C24: 1 ceramide. Biophysical journal 95, 2867-2879.

Pinto, S.N., Silva, L.C., Futerman, A.H., Prieto, M., 2011. Effect of ceramide structure on membrane biophysical properties: the role of acyl chain length and unsaturation. Biochimica et Biophysica Acta (BBA)-Biomembranes 1808, 2753-2760.

Poulos, A., Johnson, D., Beckman, K., White, I., Easton, C., 1987. Occurrence of unusual molecular species of sphingomyelin containing 28-34-carbon polyenoic fatty acids in ram spermatozoa. Biochemical journal 248, 961-964.

Rodriguez-Cuenca, S., Pellegrinelli, V., Campbell, M., Oresic, M., Vidal-Puig, A., 2017. Sphingolipids and glycerophospholipids–The "ying and yang" of lipotoxicity in metabolic diseases. Progress in lipid research 66, 14-29.

Ruiz-Argüello, M.B., Basáñez, G., Goñi, F.M., Alonso, A., 1996. Different effects of enzyme-generated ceramides and diacylglycerols in phospholipid membrane fusion and leakage. Journal of Biological Chemistry 271, 26616-26621.

Shaner, R.L., Allegood, J.C., Park, H., Wang, E., Kelly, S., Haynes, C.A., Sullards, M.C., Merrill, A.H., 2009. Quantitative analysis of sphingolipids for lipidomics using triple quadrupole and quadrupole linear ion trap mass spectrometers. Journal of lipid research 50, 1692-1707.

Slotte, J.P., 2013. Biological functions of sphingomyelins. Progress in lipid research 52, 424-437.

Sot, J., Aranda, F.J., Collado, M.-I., Goni, F.M., Alonso, A., 2005. Different effects of long-and short-chain ceramides on the gel-fluid and lamellar-hexagonal transitions of phospholipids: a calorimetric, NMR, and x-ray diffraction study. Biophysical journal 88, 3368-3380.

Sugimoto, M., Wakabayashi, M., Shimizu, Y., Yoshioka, T., Higashino, K., Numata, Y., Okuda, T., Zhao, S., Sakai, S., Igarashi, Y., 2016. Imaging mass spectrometry reveals acyl-chain-and region-specific sphingolipid metabolism in the kidneys of sphingomyelin synthase 2-deficient mice. PloS one 11, e0152191.

Takamori, S., Holt, M., Stenius, K., Lemke, E.A., Grønborg, M., Riedel, D., Urlaub, H., Schenck, S., Brügger, B., Ringler, P., 2006. Molecular anatomy of a trafficking organelle. Cell 127, 831-846.

Valsecchi, M., Mauri, L., Casellato, R., Prioni, S., Loberto, N., Prinetti, A., Chigorno, V., Sonnino, S., 2007. Ceramide and sphingomyelin species of fibroblasts and neurons in culture. Journal of lipid research 48, 417-424.

Van Meer, G., Voelker, D., Feigenson, G., 2008. Nat Rev Mol Cell Biol. Membrane lipids: where they are and how they behave 9, 112-124.

Veiga, M.P., Arrondo, J.L.R., Goni, F.M., Alonso, A., 1999. Ceramides in phospholipid membranes: effects on bilayer stability and transition to nonlamellar phases. Biophysical journal 76, 342-350.

Wang, Z., Wen, L., Zhu, F., Wang, Y., Xie, Q., Chen, Z., Li, Y., 2017. Overexpression of ceramide synthase 1 increases C18-ceramide and leads to lethal autophagy in human glioma. Oncotarget 8, 104022.

Zhang, W., Quinn, B., Barnes, S., Grabowski, G., Sun, Y., 2013. Metabolic profiling and quantification of sphingolipids by liquid chromatography-tandem mass spectrometry. J. Glycomics Lipidomics 3, 107.

Zheng, W., Kollmeyer, J., Symolon, H., Momin, A., Munter, E., Wang, E., Kelly, S., Allegood, J.C., Liu, Y., Peng, Q., 2006. Ceramides and other bioactive sphingolipid backbones in health and disease: lipidomic analysis, metabolism and roles in membrane structure, dynamics, signaling and autophagy. Biochimica et Biophysica Acta (BBA)-Biomembranes 1758, 1864-1884.

Figure Legends

Figure 1. Metabolic interconversion of ceramides and sphingomyelins.

Figure 2. (A) Heatmap representation of the relative abundance of Cer and SM in different tissues and mammalian species. (B) Heatmap representation of the relative abundance of Cer and SM in different cell lines. Each data point corresponds to the peak area of a given sphingolipid (horizontal axis) related to the sum of the peak areas of detected sphingolipids of each class. Results are averaged from a minimum of three samples (independent experiments) per data point. Actual number of samples for each data point is given under Methods. Data is expressed as percentage, as indicated in the colour code at the bottom. Grey data points indicate undetected sphingolipids. The data in figures can be found in the Supplementary Material.

Table 1. Quantification of Cer and SM most abundant species in different tissues. Quantification was achieved by comparison with authentic standards (d18:1/16:0, d18:1/18:0, and d18:1/24:1).

	RAT				HUMAN
	LIVER ng/mg	**BRAIN ng/mg**	**ADIP. T. ng/mg.**	**SERUM ng/ml**	**SERUM ng/ml**
Cer (d18:1/16:0)	4.7	0.34	2.4	52.4	67.0
Cer (d18:1/24:1)	8.6	5.7	n.d.	205.2	274.1
Cer (d18:1/18:0)	0.50	47.5	0.57	15.7	33.8
Cer (d18:1/24:0)	28.5	1.2	2.8	621.4	1173.8
SM (d18:1/16:0)	123.9	22.0	22.0	15052.3	42387.3
SM (d18:1/24:1)	64.6	95.8	3.9	9804.7	16914.1
SM (d18:1/18:0)	13.8	95.6	3.2	989.5	5312.0
SM (d18:1/24:0)	170.2	23.8	7.1	8365.1	11651.3

Table 2. Cer and SM most abundant species in different tissues (studies from other laboratories).

Tissue or cell line	SM species	Cer species	Ref
Human plasma	***C16:0***, C24:0, C22:0		(Mecatti et al., 2018)
Human synovial fluid	***C16:0***, C24:1		(Kosinska et al., 2014)
Human erythrocyte	***C16:0***, C24:1, C24:0		(Maté et al., 2014)
Human fibroblast	***C16:0***, C24:1, C24:0	***C24:1***, C16:0	(Manni et al., 2017)
Human adipose tissue	***C16:0***, C24:1, C22:0	***C24:1***, C22:0, C16:0	(Kolak et al., 2007)
Human liver nucl. Memb.	***C16:0***	***C16:0, C24:0***	(Lazzarini et al., 2015)
Human hepatoma cells	***C16:0***	***C24:0***, *C16:0*	(Lazzarini et al., 2015)
Hum. Prostate cancer	***C16:0***, C24:1, C24:0	***C24:1***, C24:0, C16:0	(Llorente et al., 2013)
Exosomes from above	***C16:0***, C24:1, C24:0	***C16:0***, C24:0, C24:1	(Llorente et al., 2013)
Hum. glioma tissue		***C18:0***	(Wang et al., 2017)
Rat cereb.granule cells	***C18:0***, C16:0	***C18:0***	(Valsecchi et al., 2007)
Mouse brain		***C18:0***	(Zhang et al., 2013)
Mouse liver	***C16:0***, C24:0, C24:1	***C24:0***, C16:0, C22:0	(Sugimoto et al., 2016)
Mouse liver		***C24:0***, C24:0, C16:0	(Zhang et al., 2013)
Mouse lung		***C24:0***, C24:1, C16:0	(Zhang et al., 2013)
Mouse lung	***C16:0***, C24:1, C24:0	***C24:0***, C24:1, C22:0	(Dautel et al., 2017)
Mouse spleen		***C24:0***, C24:1, C16:0	(Zhang et al., 2013)
Mouse muscle	***C18:0,*** C22:1, C22:0	***C18:0***	(Montgomery et al., 2017)
MDCK cells	***C16:0***, C24:1, C24:0	***C24:0,*** C24:1	(Manni et al., 2015)
DRM from above	***C16:0***, C24:1, C16:0	***C24:0,*** C24:1, C16:0	(Manni et al., 2015)

Up to three particularly abundant species are given for each sample, in order of decreasing abundance. The most abundant species for each sample is written in ***bold italics***. Only one or two species are given when they are largely predominant over any other.

Figure 1

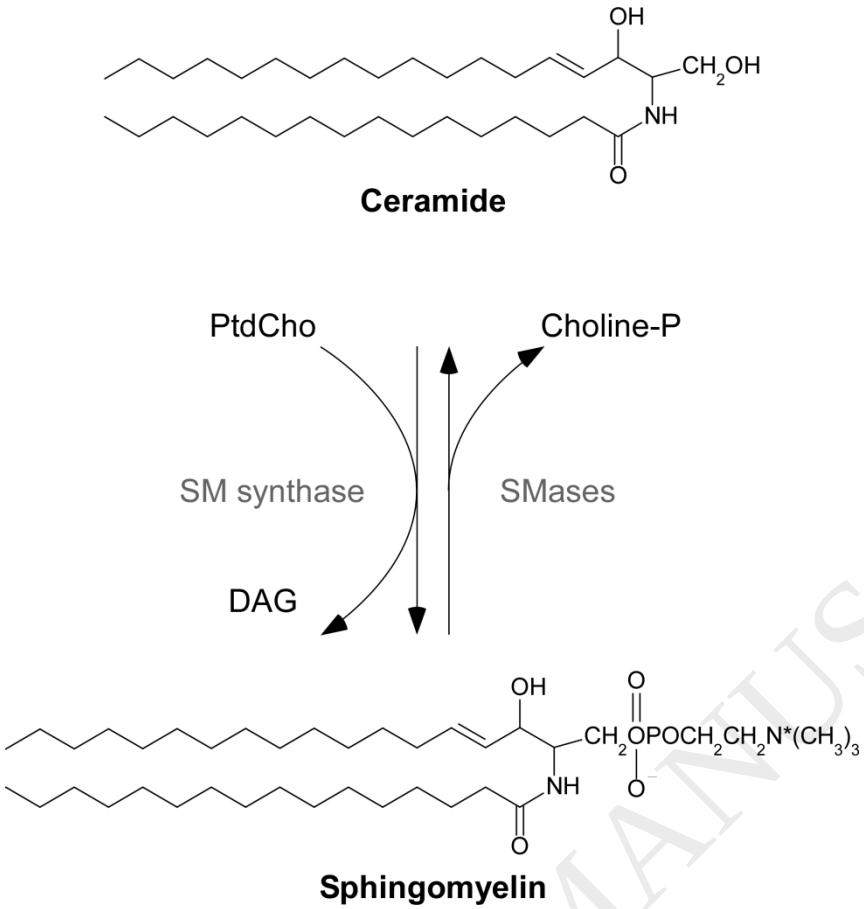

Figure 2